ACS OMEGA

http://pubs.acs.org/journal/acsodf

Article

Investigation of Dielectric, Ferroelectric, and Strain Responses of $(1 - x)[0.90(Bi_{0.5}Na_{0.5})TiO_3 - 0.10SrTiO_3] - xCuO$ Ceramics

Amir Ullah,* Amir Sohail Khan, Mahidur R. Sarker,* Muhammad Javid Iqbal, Hidayat Ullah Khan, Vineet Tirth, Ali Algahtani, and Abid Zaman*

Cite This: *ACS Omega* 2023, 8, 12372−12378

Read Online

ACCESS | Metrics & More | Article Recommendations

ABSTRACT: The low-temperature sintering of $(Bi_{0.5}Na_{0.5})TiO_3$-based ceramics can be achieved by sintering aid CuO. Piezoelectric ceramics $(1 - x)[0.90(Bi_{0.5}Na_{0.5})TiO_3 - 0.10SrTiO_3] - xCuO$ (BNT-ST-Cu) with x = 0, 0.01, 0.02, 0.03, and 0.04 were prepared through the mixed oxide route. A tetragonal structure was indexed for the undoped sample. Its structure was found to be changed to a pseudocubic when Cu was added. For undoped Cu samples, the sintering temperature (T_s) for sufficient densification was 1160 °C. However, T_s was reduced to 1090−1120 °C for Cu-added specimens. Field emission scanning electron microscopy (FE-SEM) showed a uniform and dense grain morphology for all samples. The maximum dielectric constant temperature (T_m) was decreased with the doping concentration of Cu and applied frequency. The strain was increased with Cu concentration and had the maximum value of 500 pm/V for the sample x = 0.02 with symmetric and slim strain loops.

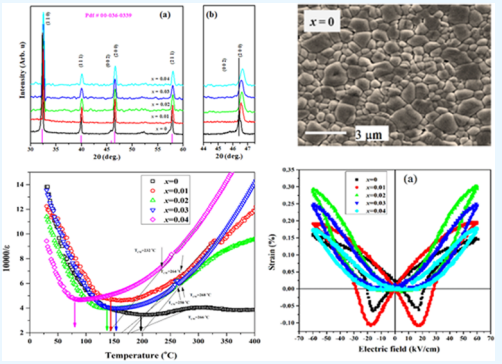

INTRODUCTION

Lead-based ceramics are widely used in commercial markets like sensors, transducers, resonators, and actuators because of their excellent strain and ferroelectric properties.[1,2] Pb is hazardous and is a threat to the environment and human health. Serious efforts are underway to remove it from all devices of Pb-based ceramics. This trend of working on lead-free ceramics is getting excellent attraction around the globe. Researchers first considered $Bi_{0.5}Na_{0.5}TiO_3$ (BNT) as a possible alternative to lead-based materials. BNT has a perovskite ABO_3 structure with rhombohedral symmetry and space group $R3C$. BNT has a high Curie temperature, T_C, of 320 °C and a high ferroelectric response (P_r = 38 μC cm^{-2}) due to which this system is considered a favorable alternative to lead-based ceramics. In view of the high coercive field (E_c = 73 kV/cm) and high conductivity, the polling process of this system becomes hard, restricting its practical utility.[3−5]

In view of their low toxicity, simplicity, and easy processing, $(K,Na)NbO_3$ (KNN) [6], NBT−$(K_{0.5}Bi_{0.5})TiO_3$ (NBT-KBT), and NBT-$BaTiO_3$ (NBT-BT) are also considered potential lead-free alternatives.[6,7] These systems have been reported to be room-temperature ferroelectrics with a morphotropic phase boundary (MPB) untying the tetragonal phase from the rhombohedral. Accompanied by the ferroelectric response, these perovskites also induce relaxation behavior.[7]

BNT systems modified with $BaTiO_3$ have exhibited good piezoelectric properties near MPB.[8−12] $SrTiO_3$ (ST) is, however, considered to be more symmetric and favorable in combination with BNT.[13,14] ST-modified BNKT has been reported to demonstrate much improved piezoelectric properties.[15] In another report, BNST100x revealed a high dynamic strain of (d^*_{33}) of 488 pm/V with x = 0.28.[16] $SrTiO_3$ has a cubic symmetry with the space group of $Pm3m$.[17] A thorough study of a BNT-based solid solution has revealed that these ceramics have lower electrical and electromechanical properties compared with those of lead-based ones. Furthermore, the compound $100 - x(Bi_{0.5}Na_{0.5})TiO_3 - xSrTiO_3$ with x = 0−9 was thoroughly studied and their electrical and electromechanical properties were investigated.[18]

The main contribution of the added CuO was considered a sintering additive. However, Jiang et al. studied the Cu-doped $(K_{0.5}Na_{0.5})NbO_3$−$MgTiO_3$ and reported improvement in the mechanical quality factor (Q_m) and ferroelectric properties.[19]

In another report, Bong et al. investigated Cu-doped $Bi_{0.5}(Na_{0.79}K_{0.21})TiO_3$ (BNKT−xCu). Cu increased the d_{33}-value up to 156 pC/N for BNKT−0.6Cu. Also, the dielectric permittivity maximum (T_m) increased gradually while the depolarization temperature (T_d) decreased during the heating and cooling cycles.[20] To drive forward this study for the

Received: January 9, 2023
Accepted: March 1, 2023
Published: March 21, 2023

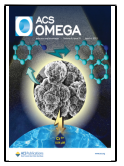

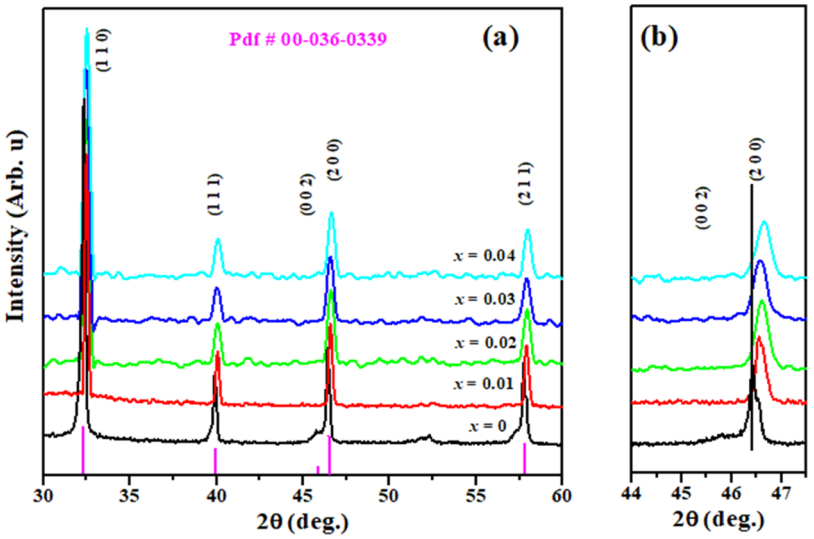

Figure 1. (a) XRD pattern of the sintered pellets of BNT-ST-Cu ceramics in the 2θ range of 30−70° and (b) enlarged view in the 2θ range 46−47°.

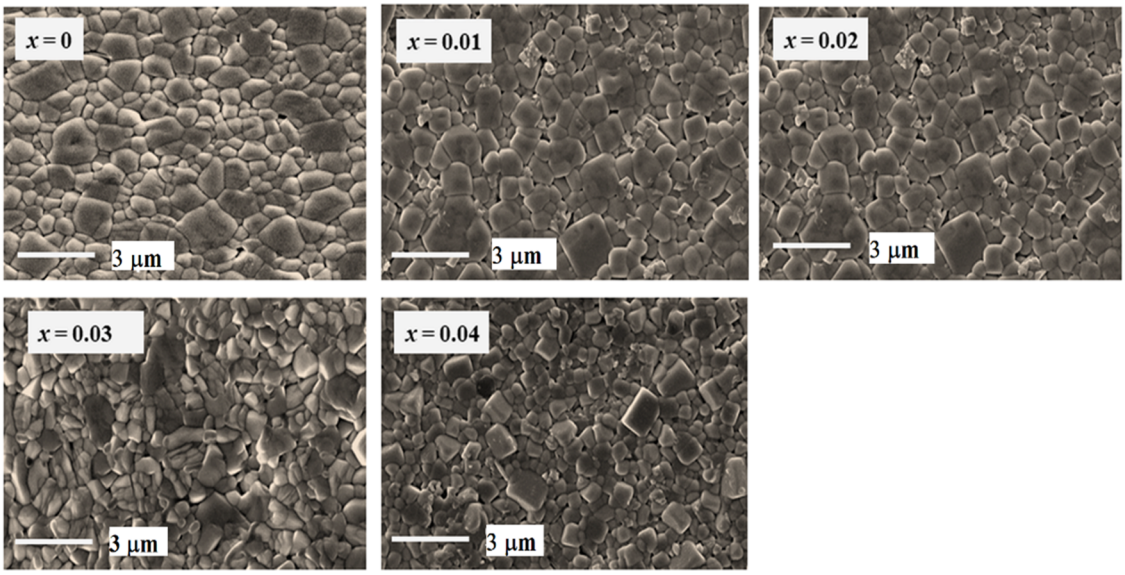

Figure 2. FE-SEM images of the BNT-ST-Cu system with Cu ratios of 0, 0.01, 0.02, 0.03, and 0.04.

improvement of electrical and electromechanical properties and to decrease the sintering temperature, the BNT system was modified with Cu.

The solid solution series of these piezoceramic systems $(1-x)[0.90(Bi_{0.5}Na_{0.5})TiO_3 - 0.10SrTiO_3]-xCuO$ (BNT-ST-Cu) (x = 0, 0.01, 0.02, 0.03, and 0.04) were prepared. In this method, ball milling is a mechanical technique that is broadly used to grind powders into fine particles and its effect on microstructural, dielectric, phase, strain, and ferroe l ectric properties development of milled powders.

RESULTS AND DISCUSSION

Figure 1 displays the X-ray diffraction (XRD) pattern of the pellets of BNT-ST-Cu ceramics in the 2θ range (30−70°). All compositions (x = 0, 0.01, 0.02, 0.03, and 0.04) revealed a perovskite having a single phase with no bits of secondary phases, indicating that Cu^{2+} is effectively replaced on the A-site of the BNT-ST-Cu lattice.[21,22] Undoped sample is indexed to be tetragonal, as is evident by the two clear split (002)/(200) peaks at the 2θ degree around 46°, which matched with the pdf card #00-036-0339. However, the two (002)/(200) peaks merged into a single intensity peak (200) at the 2θ degree around 46°, describing a pseudocubic structure. Since the ionic radius of copper (Cu) is comparable to that of Ti^{4+}, it can possibly replace the Ti^{4+} ion. The peaks were slightly shifted to a higher angle side, which indicates that the crystal volume size was decreased with the incorporation of the Cu ion on the B site (T site).[19,20] Based on the ionic radii, since the Cu concentration is quite small, there is a possibility that it diffuses into the lattice of the parent compound. Second, for all compositions, the synthesis compound displays a single phase, which is further confirmation that the Cu ion is totally diffused into the lattice of the parent compound. The effects of Cu^{2+} doping has a similar tendency to that observed for the Zr, Nb, and Sn addition in BNT-based perovskites.[23−25]

Figure 2 exhibits the FE-SEM pictures of the BNT-ST-Cu with Cu ratios of 0, 0.01, 0.02, 0.03, and 0.04. The substitution of the Cu^{2+} content resulted in changes in the grain

https://doi.org/10.1021/acsomega.3c00128
ACS Omega 2023, 8, 12372−12378

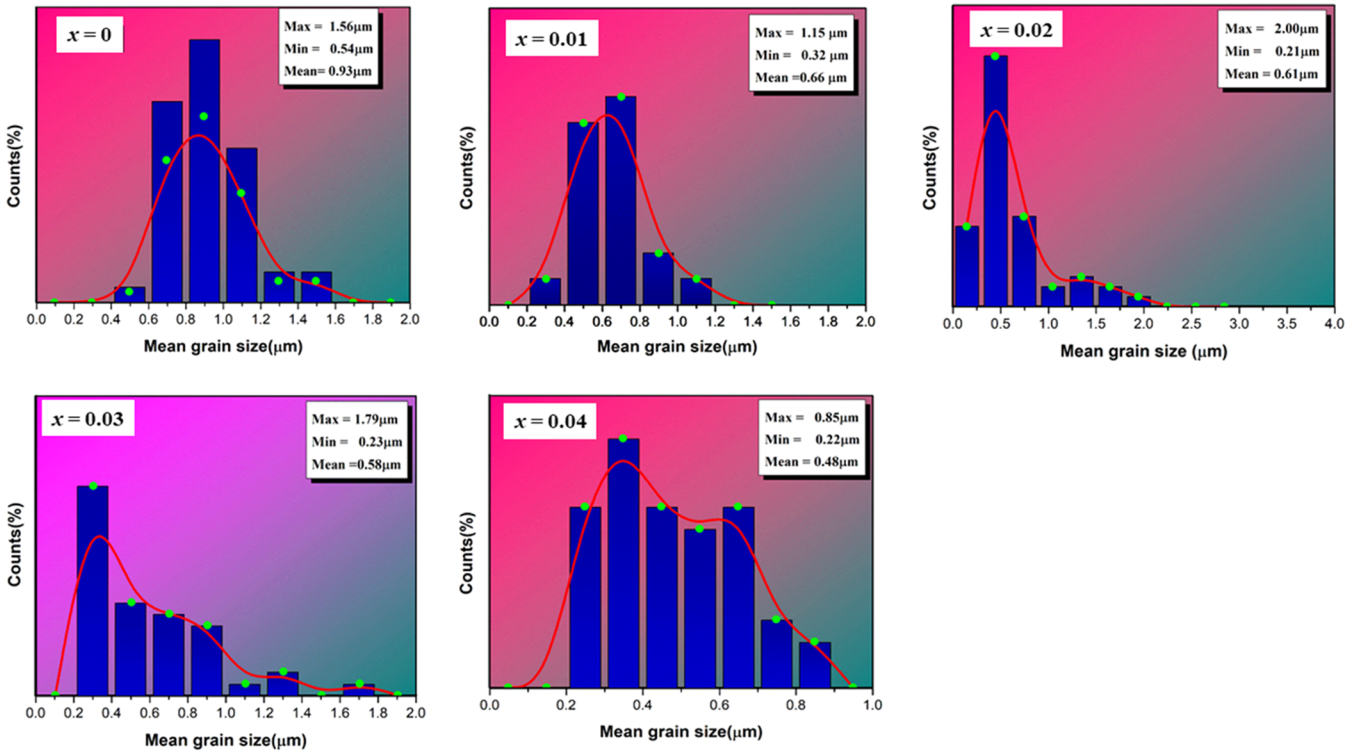

Figure 3. Histogram of the grain size of BNT-ST-Cu ceramics with Cu ratios of 0, 0.01, 0.02, 0.03, and 0.04.

Table 1. Physical and Electrical Properties of BNT-ST-Cu Ceramics Sintered at 1090 °C

BNT-ST-Cu	grain size (μm)	ρ (g/cm^3)	ΔT_m (°C)	T_m (°C)	ε	tan δ (%)	P_r (μC/cm^2)	P_{max} (μC/cm^2)	E_c (kV/cm)	d_{33}^* (pm/V)
0	0.96	5.79	68	200	790	2.2	25.7	33.7	24.6	250
0.01	0.66	5.80	100	159	954	2.4	23.7	33.1	20.0	334
0.02	0.61	5.88	130	123	899	2.8	15.4	32.7	15.0	500
0.03	0.58	5.85	104	132	936	2.7	8.6	27.4	8.0	408
0.04	0.48	5.82	153	79	1308	3.2	5.5	20.3	8.6	316

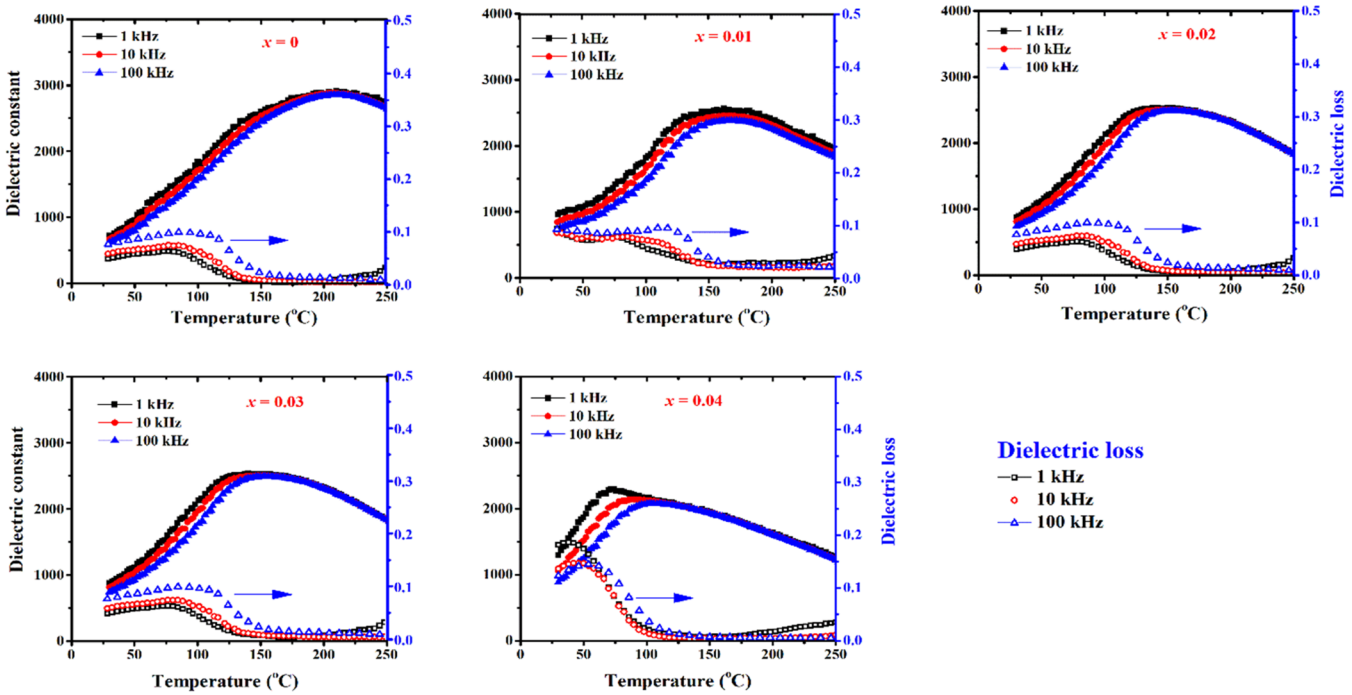

Figure 4. Dielectric constant (ε) and loss (tan δ) of the BNT-ST-Cu compound with x = 0−0.04.

https://doi.org/10.1021/acsomega.3c00128
ACS Omega 2023, 8, 12372−12378

morphology as well as average grain size. The average grain size was found with the help of the software Nanomeasure 1.2. The mean grain size of the undoped sample was found to be larger and round in shape. The round grain morphology was transformed to square and rectangular with the Cu^{2+} substitution.[26,27] This phenomenon may be due to the reaction between Cu^{2+} and sodium carbonate, which produce some melted compounds.[27]

Figure 3 shows the distribution of grain morphology of BNT-ST-Cu with Cu ratios of 0, 0.01, 0.02, 0.03, and 0.04. The average grain size of the undoped (x = 0) system was determined to be 0.93 μm. The grain size was, however, decreased to 0.66, 0.61, 0.58, and 0.48 μm, respectively, for x = 0.01, 0.02, 0.03, and 0.04. The grain density ($\langle\rangle$) of 5.79, 5.80, 5.88, 5.85, and 5.82 g/cm^3 was estimated for the samples x = 0, 0.01, 0.02, 0.03, and 0.04, respectively, also displayed in Table 1.

Figure 4 shows the plots of dielectric permittivity (ε) and loss (tan δ) vs temperature of the BNT-ST-Cu systems with Cu ratios of 0, 0.01, 0.02, 0.03, and 0.04 at selected frequencies of 1, 10, and 100 kHz. The dopant concentration affected the dielectric permittivity and loss of the BNT-ST-Cu ceramics.[28] The temperature of the maximum dielectric constant (T_m) was reduced with the increasing ratios of Cu^{2+}, and the corresponding peaks became more broadened. Peaks at T_m (arrowed) were shifted to a higher temperature side with the rise in frequency, describing the relaxor nature of the BNT-ST-Cu system. The temperature-dependent tangent loss (%) was found to be low (less than 10%) and stable up to temperature around 300 °C for samples with x = 0, 0.01, 0.02, and 250 °C for x = 0.03 and 0.04.

Using the Curie–Weiss law, the dielectric relaxation of the BNT-ST-Cu samples was explained. In the reported literature, it was described that the permittivity of a normal ferroelectric ceramic beyond the T_c must follow the Curie–Weiss law.[29]

$$\frac{1}{\varepsilon} = \frac{T - T_C}{C} (T > T_C) \quad (1)$$

In eq 1, C is the constant of the Curie–Weiss law. The converse permittivity graphs are plotted against temperature for all samples at the frequency of 10 kHz as shown in Figure 5. It was also observed that the permittivity of the BNT-ST-Cu compound diverged from the Curie–Weiss law when the Cu ratio was enhanced. The change in temperature $\Delta T_m = T_{CW} - T_m$ between the Curie–Weiss temperature and Curie temperature was taken to find out the extent of the deviation. ΔT_m was found to be 6 °C for x = 0 and 9 °C for x = 0.01, 28 °C for x = 0.02, 10 °C for x = 0.03, and 42 °C for x = 0.04 (Table 1). Hence, ΔT_m was enhanced with the incorporation of the Cu amount. This behavior in the BNT-ST-Cu ceramics indicates the relaxation and diffused phase phenomena.[30] Moreover, when the Cu amount was increased, the transformation of the diffuse–relaxor phase was enhanced.

Figure 6a,b displays the polarization vs electric field (P–E) relationship of the BNT-ST-Cu system with x = 0, 0.01, 0.02, 0.03, and 0.04 under an applied field of 60 kV/cm. For an undoped sample (x = 0), the remnant polarization (P_r), maximum polarization (P_{max}), and coercive field (E_c) were acquired to be around 25.7 μC/cm^2, 33.7 μC/cm^2, and 24.6 kV/cm, respectively. P_r, P_m, and E_c were decreased to 5.5 μC/cm^2, 20.3 μC/cm^2, and 8.6 kV/cm for sample x = 0.04. The loops then became fairly slim and saturated for Cu-doped ceramics. Doping of Cu caused the ferroelectric loops to show more relaxation accompanied by a drastic decrease in P_r and E_c, e.g., x = 0.02.[31−34]

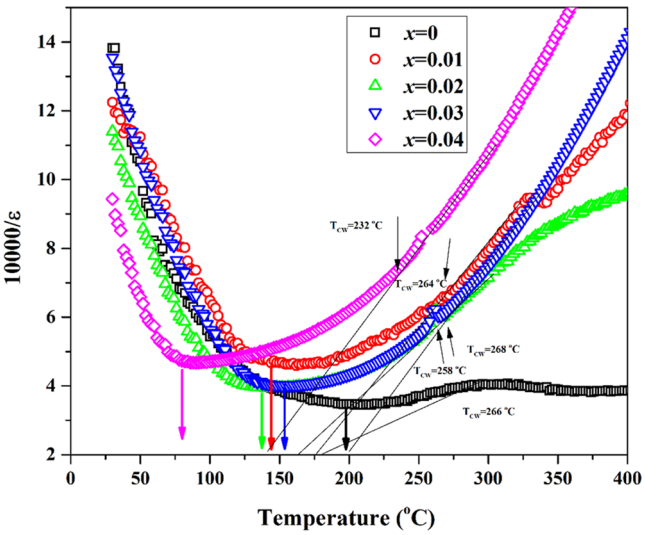

Figure 5. Converse permittivity plots versus temperature for all samples at a frequency of 10 kHz.

As shown in Figure 7, the butterfly bipolar strain of BNT-ST-Cu (x = 0, 0.01, 0.02, 0.03, and 0.04) was investigated under an electric field of 60 kV/cm. The bipolar strain (S%) found for the sample with x = 0 was 0.15% and increased for Cu^{2+} doping (0.02) up to a value of 0.30% and then reduced for further doping. Percent strain can be converted to a dynamic strain d^*_{33} = (S_{max}/E_{max}) by dividing the maximum strain over the maximum electric field. The maximum dynamic strain d^*_{33} was found to be around 500 pm/V, which is larger than the values reported in the system BNST100x.[35−37] The strain curves were found to be highly saturated with a negative strain for x = 0 and 0.01. This illustrates that Cu^{2+} ratios disrupted the ferroelectric state of the samples, causing the curves to display more relaxor behavior.[38,39] N.B. slim and symmetric loops were obtained for the entire Cu-modified series. The loops displayed low hysteretic loss in the compound. This trend agrees well with the dynamics of the dielectric constant of similar solid solutions.

Figure 8a,b is a montage of a unipolar field-dependent strain of the BNT-ST-Cu ceramics with Cu contents x = 0, 0.01, 0.02, 0.03, and 0.04 under a field of 60 kV/cm. The unipolar strain (S%) recorded from the undoped ceramic (x = 0) was 0.15% and gradually increased for Cu-doped samples. The maximum strain of 0.30% was attained for sample x = 0.02, and the strain was reduced with the further incorporation of Cu^{2+}, showing the possible disruption of the ferroelectric pattern of the system.[38,39] Percent strain can be converted to a dynamic strain d^*_{33} = (S_{max}/E_{max}) by dividing the maximum strain over the maximum electric field (Figure 8b). The highest value for the dynamic strain was 500 pm/V for the sample x = 0.02, consistent with the values recorded from BNST100x.[35−37] The strain loops are slim and symmetric for all Cu-doping values, indicating the loss of hysteretic behavior. The static d_{33} values were also found for all samples and are displayed in Figure 8b. The d_{33} value for the undoped sample x = 0 was 121 pC/N and decreased as the Cu amount was increased. As per the phenomenological theory, d_{33} can be related to the dielectric constant and the spontaneous polarization, P_s, and high P_r.[34]

https://doi.org/10.1021/acsomega.3c00128
ACS Omega 2023, 8, 12372−12378

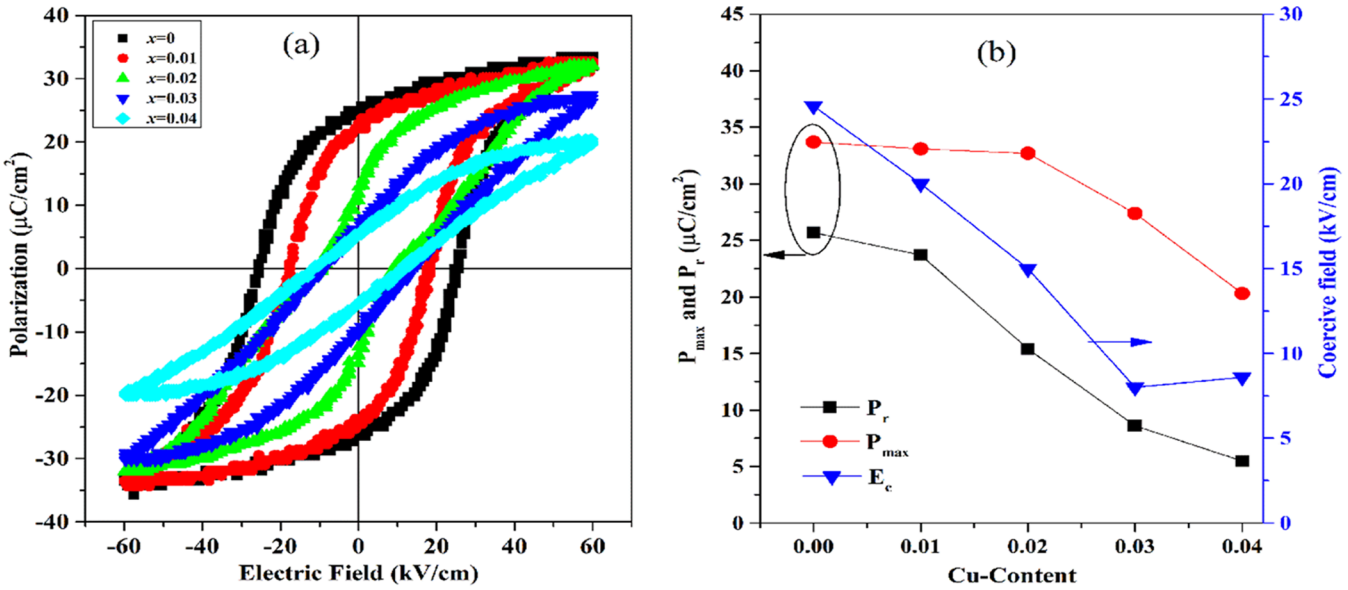

Figure 6. Ferroelectric (P−E) loops of the BNT-ST-Cu system with Cu ratios x = 0, 0.01, 0.02, 0.03, and 0.03.

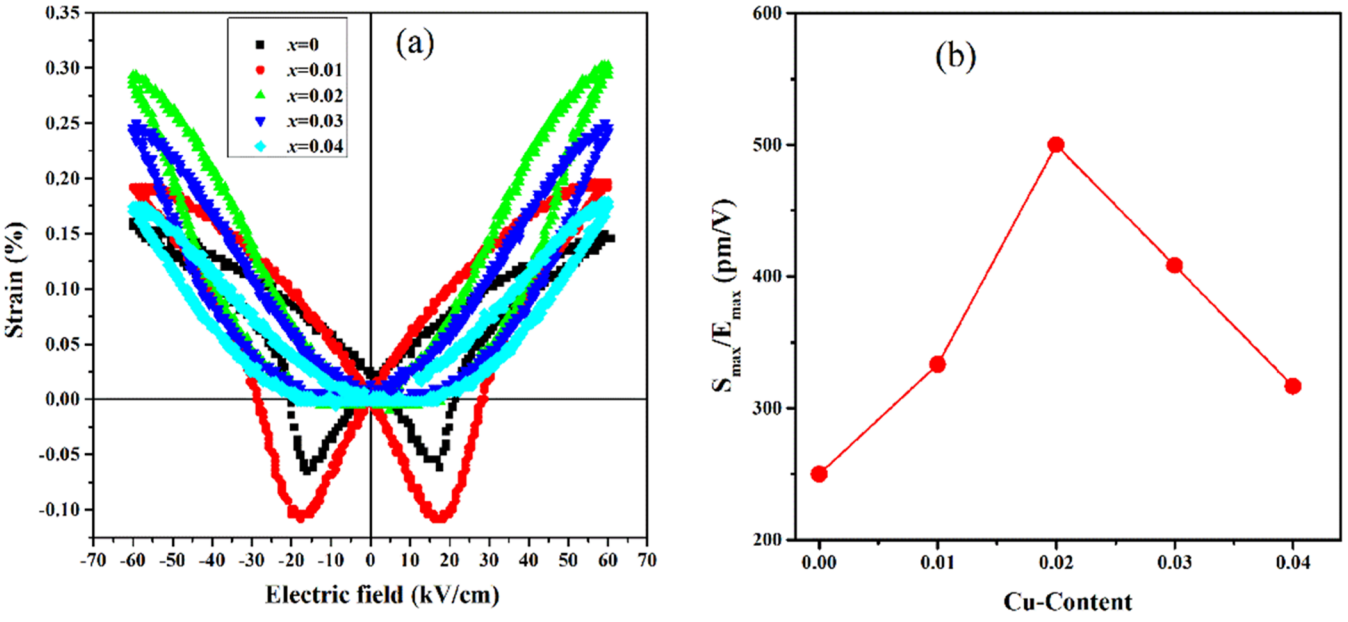

Figure 7. (a, b) Butterfly bipolar strain loops of the BNT-ST-Cu compound with x = 0, 0.01, 0.02, 0.03, and 0.04.

CONCLUSIONS

Lead-free systems $(1 - x)[0.90(Bi_{0.5}Na_{0.5})TiO_3 - 0.10SrTiO_3] - xCuO$ (BNT-ST-Cu) with x = 0, 0.01, 0.02, 0.03, and 0.04 were made via the solid solution method. The undoped sample is indexed to be tetragonal; however, a pseudocubic structure was found for samples $x \geq 0$.

For undoped Cu samples, the sintering temperature (T_s) for sufficient densification was 1160 °C. However, T_s was reduced to 1090−1120 °C for Cu-added specimens. FE-SEM demonstrated a uniform and dense grain morphology. The temperature T_m was decreased as a function of the increasing Cu content. The change in temperature $\Delta T_m = T_{CW} - T_m$ between Curie−Weiss temperature and Curie temperature was taken to find out the extent of the deviation. ΔT_m was found to be 68 °C for x = 0, 100 °C for x = 0.01, 130 °C for x = 0.02, 104 °C for x = 0.03, and 153 °C for x = 0.04. For the undoped sample (x = 0), the remnant polarization (P_r), maximum polarization (P_{max}), and coercive field (E_c) were acquired to be around 25.7 $\mu C/cm^2$, 33.7 $\mu C/cm^2$, and 24.6 kV/cm, respectively. P_r, P_{max}, and E_c were decreased to 5.5 $\mu C/cm^2$, 20.3 $\mu C/cm^2$, and 8.6 kV/cm for the sample x = 0.04, respectively. The loops were then become fairly slim and saturated for Cu-doped ceramics. A high strain of the undoped sample was found to be 0.30% with a dynamic strain value of 500 pm/V. The strain was, however, subtly decreased with the doping of Cu, making the loops symmetric and slim. This describes the onset of a relaxor ferroelectric state.

EXPERIMENTAL SETUP

Piezoelectric system BNT-ST-Cu was obtained through a simple mixed solid solution technique. Powders of Na_2CO_3, TiO_2, Bi_2O_3, (99.9% High Purity Chemicals, Japan), $SrCO_3$, and CuO_2 (99.9% Cerac Specialty In-organics) were chosen as

https://doi.org/10.1021/acsomega.3c00128
ACS Omega 2023, 8, 12372−12378

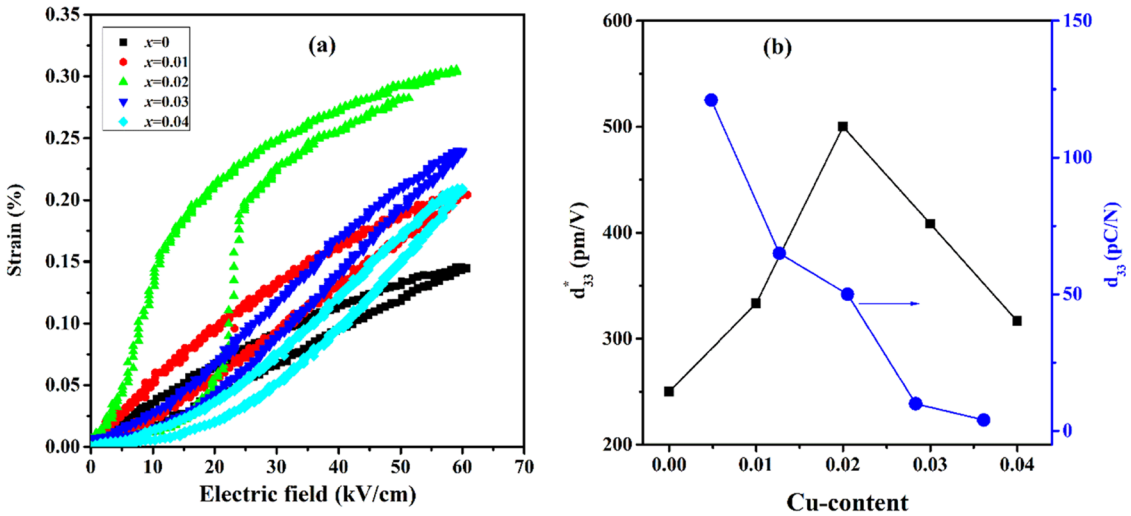

Figure 8. (a) Unipolar strain and (b) dynamic and static strains of the compound BNT-ST-Cu with Cu contents x = 0, 0.01, 0.02, 0.03, and 0.04.

the reactant powders. These raw ceramics were stoichiometrically measured and ball milled for the whole day in ethanol having zirconia media. Powders were dried at 100 °C, crushed, and calcined at about 850 °C for 02 h. The compound was then crushed into a fine powder, an aqueous poly(vinyl alcohol) (PVA) solution was added to avoid cracks in the disk, and finally, green pellets were made with a diameter of 10 mm and a thickness of 1mm at an applied stress of 120 MPa. The sintering of pellets for undoped sample x = 0 was done at a temperature of 1160 °C for 2 h. However, the pellets were sintered for Cu-doped (x = 0.04) samples even at a low temperature of 1090 °C. An X-ray diffractometer (XRD, X'Pert-PRO MRD, Philips, KBSI) was used for determining the lattice parameters and crystal structure of the as-polished pellets.

The surface microstructure study of the polished disks was obtained using a field emission scanning electron microscope (FE-SEM, Hitachi S-4200 & Japan). Electrodes were employed on the surfaces of the pellets with silver paste and annealed at 700 °C for 30 min. The polarization study was carried out at 1 frequency of 1 Hz with the help of the Sawyer−Tower circuit with an alternating electric field having a sinusoidal waveform. The strain was found at a frequency of 200 mHz by a Linear Variable Differential Transducer (LVDT, Mitutoyo MCH-331 & M401).

An external applied electric field of 30−40 kV/cm was used to pole the samples in silicon oil. An impedance analyzer (HP4192A) was used for measuring the dielectric constant of the polled samples. d_{33} meter using a quasi-static method was employed for measuring the piezoelectric constant.

AUTHOR INFORMATION

Corresponding Authors

Amir Ullah − *Department of Physics, Islamia College Peshawar, Peshawar 25120 KP, Pakistan*; Email: amirullah@icp.edu.pk

Mahidur R. Sarker − *Institute of IR 4.0, Universiti Kebangsaan Malaysia, Bangi 43600, Malaysia; Industrial Engineering and Automotive, Nebrija University, 28015 Madrid, Spain*; Email: mahidursarker@ukm.edu.my

Abid Zaman − *Department of Physics, Riphah International University, Islamabad 44000, Pakistan*; orcid.org/0000-0001-9527-479X; Email: zaman.abid87@gmail.com

Authors

Amir Sohail Khan − *Department of Energy Systems Research, Ajou University, Suwon 16499, South Korea*

Muhammad Javid Iqbal − *Department of Physics, University of Peshawar, Peshawar 25120 KP, Pakistan*

Hidayat Ullah Khan − *Department of Physics, University of Peshawar, Peshawar 25120 KP, Pakistan*

Vineet Tirth − *Mechanical Engineering Department, College of Engineering, King Khalid University, Abha 61421 Asir, Kingdom of Saudi Arabia; Research Center for Advanced Materials Science (RCAMS), King Khalid University, Guraiger, Abha 61413 Asir, Kingdom of Saudi Arabia*; orcid.org/0000-0002-8208-7183

Ali Algahtani − *Mechanical Engineering Department, College of Engineering, King Khalid University, Abha 61421 Asir, Kingdom of Saudi Arabia; Research Center for Advanced Materials Science (RCAMS), King Khalid University, Guraiger, Abha 61413 Asir, Kingdom of Saudi Arabia*

Complete contact information is available at: https://pubs.acs.org/10.1021/acsomega.3c00128

Notes

The authors declare no competing financial interest.

ACKNOWLEDGMENTS

This research was funded by the Universiti Kebangsaan Malaysia under Grant Codes GGPM-2021-050 and GP-2021-K023619, Universidad Antonio de Nebrija under Grant Code the Comunidad de Madrid [grant SEGVAUTO 4.0-CMP2018EEMT-4362], and the Agencia Estatal de Investigación [grant RETOS 2018-RTI2018-095923-B-C22]. The authors extend their appreciation to the Deanship of Scientific Research at King Khalid University Abha 61421, Asir, Kingdom of Saudi Arabia, for funding this work through the Small Groups Project under grant number RGP.1/123/43.

REFERENCES

(1) Maeder, M. D.; Damjanovic, D.; Setter, N. Lead free piezoelectric materials. *J. Electroceram.* **2004**, *13*, 385−392.

(2) Directive EU. 96/EC of the European Parliament and of the Council of 27 January 2003 on waste electrical and electronic equipment (WEEE). *Off. J. Eur. Communities: Legis.* **2002**, *L 37*, 24−38.

(3) Ullah, A.; Gul, H. B.; Ullah, A.; Sheeraz, M.; Bae, J. S.; Jo, W.; Ahn, C. W.; Kim, I. W.; Kim, T. H. Giant room-temperature electrostrictive coefficients in lead-free relaxor ferroelectric ceramics by compositional tuning. *APL Mater.* **2018**, *6*, No. 016104.
(4) Ullah, M.; Khan, H. U.; Ullah, A.; Ullah, A., III; Kim, W.; Qazi, I.; Ahmad, I. Dielectric, ferroelectric and piezoelectric properties of (1-*x*)(Bi0. 5Na0.5) 0.935 Ba0. 065Ti-*x* ($LiSbO_3$) solid solutions. *Ceram. Int.* **2018**, *44*, 556−562.
(5) Takagi, S.; Subedi, A.; Singh, D. J.; Cooper, V. R. Polar behavior of the double perovskites Bi M $ZnNbO_6$ (M= Pb and Sr) from density-functional calculations. *Phys. Rev. B* **2010**, *81*, No. 134106.
(6) Panda, P. K. Review: Environmental friendly lead-free piezoelectric materials. *J. Mater. Sci.* **2009**, *44*, 5049−5062.
(7) Eichel, R.-A.; Kungl, H. Recent developments and future perspectives of lead-free ferroelectrics. *Funct. Mater. Lett.* **2010**, *03*, 1−4.
(8) Lin, D.; Kwok, K. W. Structure and piezoelectric properties of new (Bi0.5Na0.5)1−*x*− yBa*x*(Yb0.5Na0.5)yTiO_3 lead-free ceramics. *J. Mater. Sci. Mater. Electron.* **2010**, *21*, 1119−1124.
(9) Li, J.; Wang, F.; Qin, X.; Xu, M.; Shi, W. Large electrostrictive strain in lead-free Bi0. 5Na0. 5TiO3−BaTiO3−KNbO3 ceramics. *Appl. Phys. A: Mater. Sci. Process.* **2011**, *104*, 117−122.
(10) Huang, S. L.; Guan, L. X.; Yi, J. B.; Zhao, B. C.; Wu, Yu.; Fan, Z. C.; Sum, T. C.; Ding, Jun.; Wang, Lan. Magnetic and electric transport properties of $Nd_{0.75}Sr_{1.25}Co_{1-x}$ MnxO_4. *J. Appl. Phys.* **2008**, *104*, No. 123904.
(11) Xu, M.; Wang, F.; Wang, T.; Chen, Z.; Tang, Y.; Shi, W. Phase diagram and electric properties of the (Mn, K)-modified Bi0. 5Na0. 5TiO3−BaTiO3 lead-free ceramics. *J. Mater. Sci.* **2011**, *46*, 4675−4682.
(12) Ngoc Tran, V.D.; Ullah, A.; Dinh, T. H.; Lee, J.-S. Effect of lanthanum doping on ferroelectric and strain properties of 0.96 Bi1/2(Na0. 84K0.16)1/2TiO3-0.04 $SrTiO_3$ lead-free ceramics. *J. Electron. Mater.* **2016**, *45*, 2639−2643.
(13) Hiruma, Y.; Imai, Y.; Watanabe, Y.; Nagata, H.; Takenaka, T. Large electrostrain near the phase transition temperature of (Bi0.5Na0.5)TiO3−$SrTiO_3$ ferroelectric ceramics. *Appl. Phys. Lett.* **2008**, *92*, No. 262904.
(14) Ijuu, D.; Kimura, T.; Yamada, T.; Funakubo, H. Preparation and Characteristics of Bi0. 5Na0. 5TiO3 Single-Crystalline Films by a Solid-State Process. *J. Am. Ceram. Soc.* **2011**, *94*, 3291−3295.
(15) Ahmed Malik, R.; Hussain, A.; Zaman, A.; Maqbool, A.; Rahman, J. U.; Song, T. K.; Kim, W.-J.; Kim, M.-H. Structure−property relationship in lead-free A-and B-site co-doped Bi0.5-(Na0.84K0.16)0.5TiO3−SrTiO3 incipient piezoceramics. *RSC Adv.* **2015**, *5*, 96953−96964.
(16) Parija, B.; Rout, S. K.; Cavalcante, L. S.; Simões, A. Z.; et al. Structure, microstructure and dielectric properties of 100− x (Bi0.5Na0.5)TiO3−*x*[SrTiO3] composites ceramics. *Appl. Phys. A* **2012**, *109*, 715−723.
(17) Fuentes, S.; Zarate, R. A.; Chavez, E.; Munoz, P.; Díaz-Droguett, D.; Leyton, P. Preparation of $SrTiO_3$ nanomaterial by a sol−gel-hydrothermal method. *J. Mater. Sci.* **2010**, *45*, 1448−1452.
(18) Waqar-Haider-Khan; Khan, A. S.; Ahmad, T.; Novak, N.; Song, X.-Q.; Saddiq, G.; Ullah, B. Unconventional high permittivity and relaxor like anomaly in (Sr,Ce, Pr)TiO3 solid solution. *J. Mater. Sci.: Mater. Electron.* **2019**, *30*, 20345−20353.
(19) Jiang, M.; Li, X.; Liu, J.; Zhu, J.; Zhu, X.; Li, L.; Chen, Q.; Zhu, J.; Xiao, D. Structural and electrical properties of Cu-doped (K0.5Na0.5)NbO3-MgTiO3 lead-free ceramics. *J. Alloys Comp.* **2009**, *479*, L18−L21.
(20) Lim, J. B.; Suvorov, D.; Jeon, J.-H. Ferroelectric Bi (Na, K)TiO3-based materials for lead-free piezoelectrics. *Ceram. Int.* **2012**, *38*, S355−S358.
(21) Shrout, T. R.; Shujun, J. Z. Lead-free piezoelectric ceramics: Alternatives for PZT. *J. Electroceram.* **2007**, *19*, 113−126.
(22) Ullah, A.; Ahn, C. W.; Ullah, A.; Kim, I. W. Large strain under a low electric field in lead-free bismuth-based piezoelectrics. *Appl. Phys. Lett.* **2013**, *103*, No. 022906.
(23) Shannon, R. D. Revised effective ionic radii and systematic studies of interatomic distances in halides and chalcogenides. *Acta Cryst. A* **1976**, *32*, 751−767.
(24) Zhang, Y.; Chu, R.; Xu, Z.; Hao, J.; Chen, Q.; Peng, F.; Li, W.; Li, G.; Yin, Q. Piezoelectric and dielectric properties of Sm2O3-doped 0.82Bi0.5Na0.5TiO3−0.18Bi0.5K0.5TiO_3 ceramics. *J. Alloys Compd.* **2010**, *502*, 341−345.
(25) Lee, J.-S.; Pham, K.-N.; Han, H.-S.; Lee, H.-B.; Tran, V. D. N. Strain enhancement of lead-free Bi1/2(Na0.82K0.18)1/2TiO3 ceramics by Sn doping. *J. Korean Phys. Soc.* **2012**, *60*, 212−215.
(26) Ullah, M.; Ullah, A.; Khan, H. U.; Ahmad, I.; Kim, I. W. Dielectric, Ferroelectric and Strain Properties of (Bi0.5Na0.5)-0.935Ba0.065Ti1−*x*(Al0. 5Nb0.5)*x*O3 Lead-free Piezoelectric Ceramics. *J. Korean Phys. Soc.* **2020**, *76*, 145−149.
(27) Gou, Q.; Wu, J.; Li, A.; Wu, B.; Xiao, D.; Zhu, J. Enhanced d33 value of Bi0. 5Na0. 5TiO3−(Ba0. 85Ca0. 15)(Ti0. 90Zr0. 10) O3 lead-free ceramics. *J. Alloys Compd.* **2012**, *521*, 4−7.
(28) Glaum, J.; Simons, H.; Acosta, M.; Hoffman, M. Tailoring the piezoelectric and relaxor properties of (Bi 1/2 Na 1/2) TiO3−BaTiO3 via Zirconium doping. *J. Am. Ceram. Soc.* **2013**, *96*, 2881−2886.
(29) Liang, S.; Zhu, J.; Zheng, M.; Zhang, P.; Sun, P.; Wang, Z.; Zhu, X. Microstructure and electrical properties of (Na0.5K0.5)1−2*x*Mg*x*NbO3−Bi0.5Na0.5TiO3 lead-free piezoelectric ceramics. *Ceram. Int.* **2014**, *40*, 2763−2768.
(30) Khan, A. S.; Ullah, B.; Novak, N.; Khan, H.; Ullah, A. Relaxor ferroelectricity and low microwave dielectric permittivity of Sr(1-*x*)Ce*x*Ti1-2/3y) MgyO3 ceramics. *Ceram. Int.* **2022**, *48*, 19434−19443.
(31) Rödel, J.; Jo, W.; Seifert, K. T. P.; Anton, E.-M.; Granzow, T.; Damjanovic, D. Perspective on the development of lead-free piezoceramics. *J. Am. Ceram. Soc.* **2009**, *92*, 1153−1177.
(32) Ullah, A.; Ullah, A.; Kim, I. W.; Lee, D. S.; Jeong, S. J.; Ahn, C. W. Large electromechanical response in lead-free La-doped BNKT−BST piezoelectric ceramics. *J. Am. Ceram. Soc.* **2014**, *97*, 2471−2478.
(33) Ullah, M.; Khan, H. U.; Ullah, A.; Ullah, A.; Won Kim, I.; Qazi, I.; Ahmad, I. Dielectric, ferroelectric and piezoelectric properties of (1-*x*)(Bi0. 5Na0.5)0.935Ba0.065Ti-*x*(LiSbO3) solid solutions. *Ceram. Int.* **2018**, *44*, 556−562.
(34) Ullah, A.; Ahn, C. W.; Malik, R. A.; Lee, J. S.; Kim, I. W. Electromechanical and microstructural study of (1-*x*)Bi0.5-(Na0.40K0.10)TiO3-*x*(Ba0.70Sr0.30)TiO3 lead-free piezoelectric ceramics. *J. Electroceram.* **2014**, *33*, 187−194.
(35) Izumi, M.; Yamamoto, K.; Suzuki, M.; Noguchi, Y.; Miyayama, M. Large electric-field-induced strain in Bi0.5Na0.5TiO3−Bi0.5K0.5-TiO3 solid solution single crystals. *Appl. Phys. Lett.* **2008**, *93*, No. 242903.
(36) Yu, Z.; Krstic, V. D.; Mukherjee, B. K. Microstructure and properties of lead-free (Bi1/2Na1/2)TiO3 based piezoelectric ceramics doped with different cations. *J. Mater. Sci.* **2007**, *42*, 3544−3551.
(37) Hiruma, Y.; Imai, Y.; Watanabe, Y.; Nagata, H.; Takenaka, T. Large electrostrain near the phase transition temperature of (Bi0.5Na0.5)TiO3−Sr TiO3 ferroelectric ceramics. *Appl. Phys. Lett.* **2008**, *92*, No. 262904.
(38) Singh, A.; Chatterjee, R. Structural, electrical, and strain properties of stoichiometric 1−*x*−y(Bi0.5Na0.5)TiO3−*x*(Bi0.5K0.5-TiO3)−y(Na0.5K0.5)NbO3 solid solutions. *J. Appl. Phys.* **2011**, *109*, No. 024105.
(39) Eitel, R. E.; Randall, C. A.; Shrout, T. R.; Park, S.-E. Preparation and characterization of high temperature perovskite ferroelectrics in the solid-solution (1-*x*)BiScO3−*x*PbTiO3. *Jpn. J. Appl. Phys.* **2002**, *41*, 2099.

https://doi.org/10.1021/acsomega.3c00128
ACS Omega 2023, 8, 12372−12378